International Journal of Engineering Trends and Technology
ISSN: 2231 – 5381 /doi:10.14445/22315381/IJETT-V69I4P225

Volume 69 Issue 4, 177-182, April 2021

Distinct Buckling Modes In Mechanical Metamaterials With Stiff Square Networks And Periodically Arranged Voids

Peter Nikitin[#], Ivan Smirnov[#], Slava Slesarenko[#1]

[#]*Saint Petersburg State University, Universitetskiy pr 28, Saint Petersburg, Russia*

[1]v.slesarenko@spbu.ru

***Abstract** – Extreme properties of mechanical metamaterials originate in their involved internal architecture. Instability-driven metamaterials harness the phenomenon of elastic buckling accompanied by significant reconfigurations of the architecture to facilitate the variability of their properties. Two common geometrical motifs often used in the design of instability-driven metamaterials are periodically arranged voids embedded into a soft deformable matrix and stiff periodic lattices with different architectures. Here the buckling behavior of metamaterials that combine these two design ideas is studied. By employing the Bloch-Floquet approach, it is demonstrated that the involved interplay between two periodic patterns significantly affects the critical strain values corresponding to the onset of instability. Moreover, two distinct buckling modes defined by the number of periodically arranged voids in the unit cell are observed. If the unit cell contains an even number of voids, then the local mode accompanied by equivalent reconfiguration in every unit cell is realized. However, if the unit cell contains an odd number of voids, then metamaterial acquires new periodicity via the formation of alternating patterns. The observed interplay between two periodic systems within one metamaterial can be further employed for more advanced designs to control the propagation of elastic waves.*

Keywords: *buckling; elastic instabilities; mechanical metamaterials; reconfiguration; structure*

I. INTRODUCTION

The first structures classified as mechanical metamaterials are so-called pentamode extreme materials proposed in 1995 [1]. These classical pentamode metamaterials assembled from the repeating unit cells combine extremely low shear modulus with a high bulk modulus, resulting in their fluid-like mechanical behavior. Despite more than 25 years of development, the most novel mechanical metamaterials employ similar fundamental design principles [2]. Their extreme properties originate in the sophisticated internal architecture, usually assembled from the repeating unit cells [3]. The rational selection of the internal architecture enables the creation of a variety of mechanical metamaterials that demonstrate very high stiffness [4], negative Poisson's ratio [5,6], or capacity to harness elastic energy [7]. Moreover, the periodic structure can give rise to the unconventional properties associated with the propagation of elastic and acoustic waves [8,9]. For metamaterials with various designs, such phenomena as the formation of bandgaps [10], negative refraction [11,12], or superlensing [13] were reported. These metamaterials often employ composite microstructure. The interplay between constituents with different properties results in the enhanced performance of the composites [14–16].

Traditionally, mechanical metamaterials, despite very involved behavior, have one fundamental weakness—their mechanical properties usually cannot be altered after fabrication. Taking into account current trends in the development of adaptive materials, there is a particular interest in creating reconfigurable mechanical metamaterials that can alter their internal architecture and properties in response to external stimuli [17]. In recent years, various types of reconfigurable mechanical and acoustic metamaterials inspired by principles of origami and kirigami have been presented [18,19]. These three-dimensional structures capable of changing their geometry in response to mechanical actuation can be employed as waveguides to control acoustic waves [20]. At the same time, such structures are very challenging for manufacturing and, moreover, are poorly scalable. A fundamentally different approach of transforming external mechanical stimuli into the reconfiguration of the internal structure exploits the phenomenon of elastic buckling [21–24]. Indeed, while elastic buckling is strongly undesirable for classical engineering materials, it is accompanied by significant displacements and changes in geometry that can be employed in the design of mechanical metamaterials [25]. This phenomenon is especially pronounced in composite materials with hyperelastic constituents capable of withstanding large deformations [26,27]. By employing the geometrical reconfigurations associated with loss of stability, it is possible not only to reversibly change the mechanical behavior of metamaterials but also to control the propagation of elastic and acoustic waves [28,29]. Since elastic waves are sensitive to the internal periodicity of the structure [30,31] and internal stress fields [10], various designs of elastic metamaterials with tunable bandgaps have been recently demonstrated. Tunability of the bandgaps/stopbands in such metamaterials were achieved, in particular, by the instability-induced formation of wavy interfaces [24,32–35]. Moreover, by employing a composite structure with stiff inclusions embedded into the soft hyperelastic matrix, it seems possible to create materials with controlled auxeticity and tunable bandgap characteristics simultaneously [6].

Among the variety of instability-driven mechanical metamaterials, two main design ideas can be often observed. The first type of mechanical metamaterials relies on the periodically distributed voids in a soft deformable matrix [30,36]. Metamaterials of the second type consist of stiff elements or networks embedded into a soft matrix [10,31]. This manuscript demonstrates that a combination of these two ideas enables the creation of mechanical metamaterials with two different types of buckling modes.

II. MATERIALS AND METHODS

A. Geometry and mechanical properties of metamaterials

Fig. 1 shows a metamaterial with the stiff square network embedded into the soft deformable matrix with voids. The lattice period a, the width of stiff struts t, the volume fraction of periodically arranged circular voids v_f and number of voids within a single unit cell n^2 univocally define the geometry of the metamaterial. The struts and matrix were considered to be hyperelastic materials with neo-Hookean strain energy density

$$W = 0.5\mu(I_1 - 3) - \mu \ln(J) + 0.5\lambda(\ln(J))^2,$$

where I_1 and J are the first and third invariants of the right Cauchy-Green deformation tensor, μ and λ are the Lame constants. Subscripts N and M stand for network and matrix, respectively. The materials are assumed to be nearly incompressible, so $\frac{\lambda_M}{\mu_M} = \frac{\lambda_N}{\mu_N} = 100$, while $\mu_c = \mu_N/\mu_M > 1$.

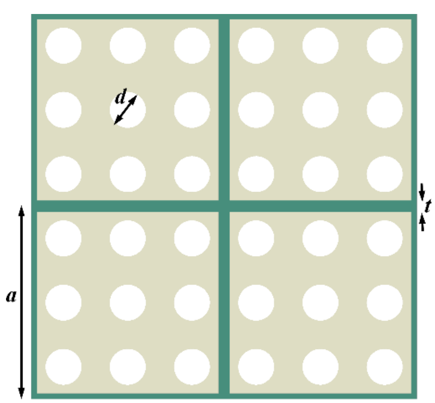

Fig. 1. Four unit cells of the considered metamaterials with stiff square networks and voids.

B. Search for instabilities

To search for the onset of instability the finite element (FE) software COMSOL 5.4 was utilized. FE analysis is a very common method in mechanical and civil engineering, enabling one to predict the properties of complex structures [37]. Since the buckling of the considered metamaterials may lead to the formation of new periodicity with a larger lattice parameter, the analysis based on the Bloch-Floquet approach was employed using the following procedure [30].

1. The primitive unit cell in the undeformed state was identified (see insert in Fig. 2).
2. The selected unit cell was subjected to equibiaxial compression by applying the following periodic boundary conditions:

$$\begin{cases} u|_{left} - u|_{right} = \varepsilon a \\ v|_{left} - v|_{right} = 0 \\ u|_{bottom} - u|_{top} = 0 \\ v_{|bottom} - v|_{top} = \varepsilon a \end{cases},$$

where u and v are horizontal and vertical displacements, respectively, a is the period of a square lattice, and ε is the applied strain (positive for compression).
3. For the obtained deformed state, a sweep along the perimeter of the IBZ was performed to compute dispersion relations $\omega(\boldsymbol{k})$, where ω is the eigenfrequency for the corresponding wavevector $\boldsymbol{k}$ at the IBZ contour (see insert in Fig. 2) [38]. To this end, Bloch-Floquet conditions were superimposed on the finitely deformed metamaterials using the following equations on the primitive unit cell boundaries:

$$\begin{cases} u_{right} = u_{left} e^{-ik_x a} \\ v_{right} = v_{left} e^{-ik_x a} \\ u_{top} = u_{bottom} e^{-ik_y a} \\ v_{top} = v_{bottom} e^{-ik_y a} \end{cases}$$

where k_x and k_y are the components of wavevector $\boldsymbol{k}$.
4. If $\omega(\boldsymbol{k}) > 0$ for all wavevectors $\boldsymbol{k}$ except for the trivial one $\boldsymbol{k} = (0,0)$, then the material remains stable at the strain ε.
5. The steps 2-4 were repeated with gradually increasing applied strain ε until the non-trivial $\boldsymbol{k_{cr}}$ with $\omega(\boldsymbol{k_{cr}}) = 0$ is found. The determined $\varepsilon_{cr} = \varepsilon$ and $\boldsymbol{k_{cr}}$ are the critical strain and critical eigenmode, respectively, corresponding to the onset of instabilities.

III. RESULTS

A. Metamaterials with a singular void within the unit cell

Elastic waves are sensitive to the geometry of the metamaterials and the internal stress state. As a result, equi-biaxial compression leads to the evolution of the dispersion curves with an increase in applied strain. Fig. 2 shows the lowest branches of the dispersion curves calculated for the vectors $\boldsymbol{k}$ at the IBZ contour (see insert in Fig. 2) for various levels of applied strain. As one can see, for applied strain ε =3.3%, the first eigenvalue at the point M is zero, reflecting the onset of instability. Since zero eigenfrequency is observed not in the origin of IBZ, new periodicity is formed, as shown in Fig. 3. The updated unit cell is four times larger than the initial unit cell and is characterized by the alternating pattern for voids.

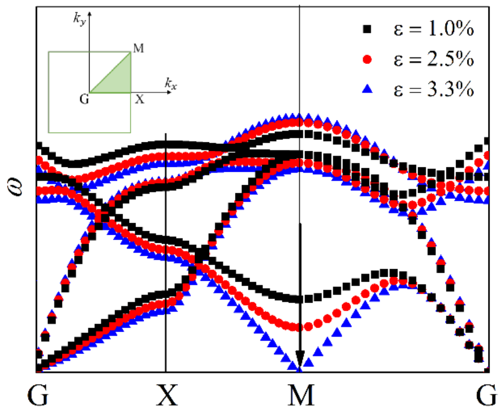

Fig. 2. Dispersion curves in the vicinity of instability for metamaterial with singular void and $v_f = 0.25$, $t = 0.02$, $\mu_N/\mu_M = 35$. Insert shows Irreducible Brillouin Zone (IBZ)

This observation is consisted with already reported results for the instability-driven metamaterials without stiff square networks. Fig. 4 shows the dependencies of the critical buckling strain on the volume fraction of the voids in the metamaterials with singular central voids and stiff square lattice. Even for the case $\mu_N = \mu_M$, corresponding to the metamaterial without networks, critical buckling strain non-monotonically depends on the volume fraction of the voids. Note that due to geometrical restrictions, the volume fraction of the voids cannot exceed $v_f^{mzx} = \pi/4$ for the metamaterial without stiff network and $v_f^{max} = \pi\left(\frac{a-t}{2a}\right)^2$ if network struts have the thickness t. One can see that with an increase in the contrast between the elastic modulus of the stiff network and soft matrix, the metamaterials become less stable regardless of the volume fraction of voids. At the same time, this effect is not very pronounced for the metamaterials with relatively small or large v_f. Moreover, for $v_f \to v_f^{max}$, the value of the critical strain is close to the value of the critical strain observed in the square networks in the absence of any soft matrix.

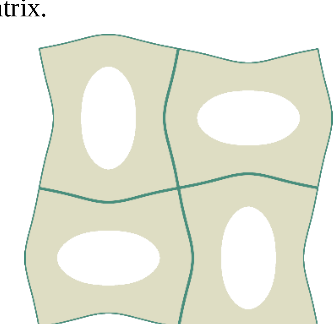

Fig. 3. The alternating buckling mode for the metamaterial with a singular void in the unit cell.

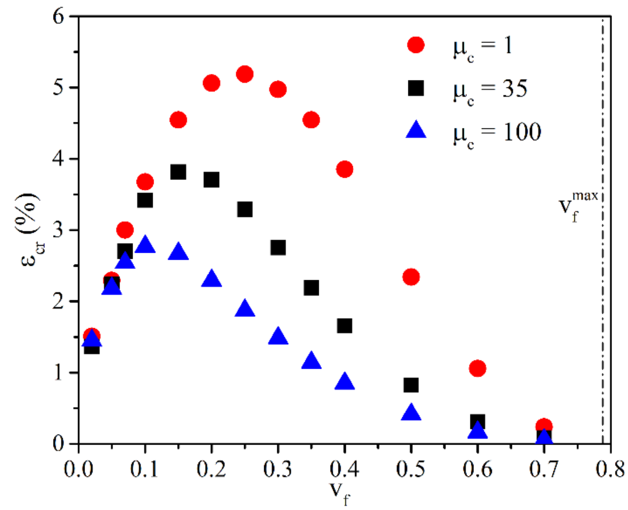

Fig. 4. Dependencies of the buckling strain on the volume fraction of the voids in the metamaterial with a singular void in the unit cell and $t = 0.02$.

Therefore, one can see that for the small v_f, the loss of stability in considered metamaterials is guided mainly by the voids, while for the large values of v_f, the stiff network plays the dominant role. By defining the maximum on the curve as the transition between the void-dominated and network-dominated buckling, it can be concluded that the increase in the elastic modulus contrast leads to a more prominent contribution of the stiff networks to the bucking process for the same v_f.

B. Metamaterials with multiple voids in one unit cell

Here the metamaterials with multiple voids $(n \times n)$ arranged in the square lattice with smaller period a/n are considered (Fig. 1). The volume fraction of the voids remains the same, while the diameter of the voids decreases with an increase in their number. Note that for the truly periodic arrangement of the voids throughout the whole infinite specimen, the number of voids cannot exceed a critical value n^{max} to avoid intersection with the stiff network, that can be determined from geometry as $n^{max} = \left\lfloor \frac{a}{t}\left(1 - 2\sqrt{\frac{v_f}{\pi}}\right)\right\rfloor$.

Search for the onset of instabilities in the metamaterials with multiple voids reveals the sufficient difference between metamaterials with odd and even number of voids located in the single unit cell. The evolution of the dispersion curves for the unit cells with an odd number of voids is similar to the case considered above. The first non-trivial zero eigenvalue corresponds to the point M at the IBZ contour ($\omega(M) = 0$). As a result, the period of the metamaterial increases two-fold in each direction, and the area of the updated unit cell is four times larger as compared with the initial state (Fig. 6a).

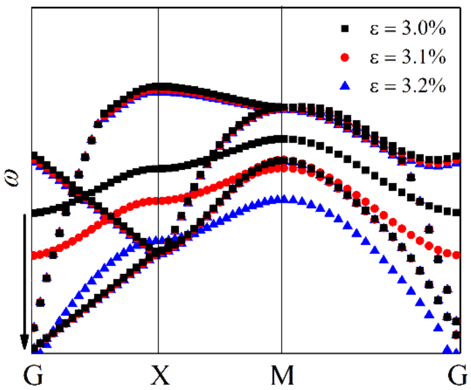

Fig. 5. Dispersion curves in the vicinity of instability for metamaterial with $n = 4$ and $v_f = 0.25$, $t = 0.02$.

At the same time, the dispersion curves for the metamaterial with an even number of voids in the unit cell demonstrate very different behavior. Fig. 5 shows the two lowest branches for the various applied strains. One may see that the second branch at the origin point G reaches zero ($\omega(G) = 0$) for strain $\varepsilon = 3.2\%$ while $\omega(M) > 0$. The eigenmodes corresponding to the vector $\boldsymbol{k} = (0,0)$ have the same periodicity as the initial metamaterial, and the unit cell keeps its size after buckling, while the local reconfigurations occur within the matrix as shown in Fig. 6b. To avoid ambiguity, the mode of buckling associated with the change in the periodicity is defined as alternating mode (Fig. 6a). In contrast, local mode corresponds to local reconfiguration within the unit cell (Fig. 6b).

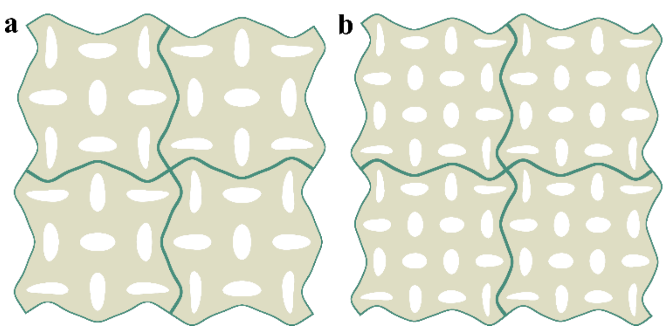

Fig. 6. Alternating (a) and local (b) buckling modes.

Employed Bloch-Floquet approach enables us to continue the analysis even beyond the onset of instabilities. Therefore the critical strains for the alternating patterns corresponding to $\omega(M) = 0$ can be obtained even in the metamaterials with an even number of voids. Fig. 7 shows the dependencies of the onsets of instabilities on the number of voids in horizontal or vertical directions within the unit cell. Square and circle symbols represent the first and the second-lowest values of the strains with either $\omega(M)$ or $\omega(G)$ equal to zero, respectively, while the interior of the symbols reflects the buckling mode. For the extreme case of $\mu_M = \mu_N$, in the absence of a stiff network due to the periodicity of the void arrangement, the critical strain does not depend on the number of voids (dashed line). Indeed, regardless of the number of voids, the metamaterials can be scaled up or down, such as the geometrical relationship between the period of the pattern and the diameter of the voids remains the same.

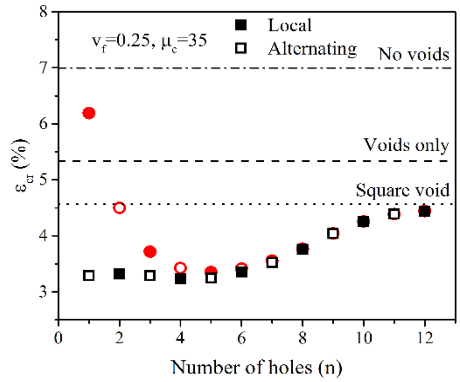

Fig. 7. Dependencies of the buckling strains for local (filled) and alternative (open) patterns on the number of voids within the unit cell (n^2).

The addition of the stiff network ($\mu \neq \mu_M$) breaks the scaling law. Similar to the metamaterial with a single void (Fig. 4), stiff networks lead to the decrease in the value of primary critical strain regardless of the number of voids (Fig. 7). However, here the primary buckling mode is univocally determined by the parity. Simultaneously, the difference between two critical strains decreases with an increase in the number of voids. For instance, while the difference between primary and secondary buckling strains for metamaterials with $v_f = 0.25$ and $\mu_N/\mu_M = 35$ is 2.9% if only a singular void is located in the middle of the unit cell, the critical strains in the metamaterial with the same geometrical and material parameters and 144 voids differ only by 0.05%. It means that in practical applications, various imperfections associated with the manufacturing process or with misaligned loading may affect the primary buckling mode in considered mechanical metamaterials. Fig. 7 also reveals that the critical strain non-monotonously depends on the number of voids. With an increase in the number of voids in the unit cells, it tends to some threshold value (dotted horizontal line).

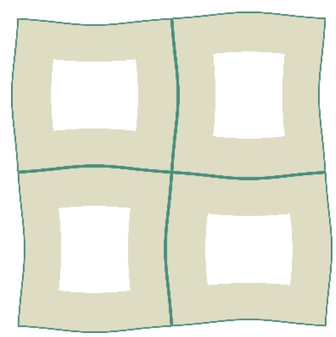

Fig. 8. Buckling mode in metamaterial with stiff square networks and square voids.

It is determined that this threshold strain corresponds to the onset of instabilities in the metamaterial with a singular square void in the center, assuming the same volume fraction of the voids (Fig. 8). Such metamaterial can be treated as the traditional square lattice with modified struts, however, the critical strain in this case is always lower as compared to the stiff network embedded into a continuous matrix without any voids (dash-dotted horizontal line in Fig. 7). The fact that buckling strain in the metamaterial with multiple voids with decreasing diameter tends to the buckling strain in the metamaterial with a single square void requires further investigation with the employment of homogenization techniques. This question is beyond the scope of the current research and will be considered in the future.

IV. CONCLUSIONS

Here, two classical motifs often found in the instability-driven mechanical metamaterials were combined. It was demonstrated that the involved interplay between stiff square networks and periodically arranged voids leads to the formation of two types of buckling patterns. If the unit cell in an undeformed state contains an even number of voids, then buckling keeps the overall periodicity, and only local changes within the unit cell are observed. At the same time, for the unit cell containing an odd number of voids, the buckling leads to a change in the periodicity accompanied by the formation of the alternating pattern. The critical buckling strains generally depend on the geometrical and materials characteristics, however, these dependencies are non-monotonous. In particular, for metamaterial with stiff square lattice and a singular void, an increase in the void diameter leads to the transition between void-dominant and network-dominant regimes, affecting the sensitivity of the buckling strain to the elastic modulus contrast. The rich design space and non-trivial instability-driven reconfigurations open new avenues for advanced metamaterials that can be employed to control the propagation of the elastic waves.

ACKNOWLEDGEMENT

This research was funded by the Russian Scientific Foundation, grant number 20-71-00017

REFERENCES

[1] Milton GW, Cherkaev AV. Which Elasticity Tensors are Realizable? Journal of Engineering Materials and Technology 117(1995) 483–93.

[2] Kadic M, Bückmann T, Schittny R, Wegener M. Metamaterials beyond electromagnetism. Reports on Progress in Physics 76(2013) 126501

[3] Zadpoor AA. Mechanical meta-materials. Materials Horizons 3(2016) 371–81.

[4] Zheng X, Lee H, Weisgraber TH, Shusteff M, DeOtte J, Duoss EB, et al. Ultralight, ultrastiff mechanical metamaterials. Science 344(2014) 1373–7.

[5] Kolken HMA, Zadpoor AA. Auxetic mechanical metamaterials. RSC Advances 7(2017) 5111–29.

[6] Li J, Slesarenko V, Rudykh S. Auxetic multiphase soft composite material design through instabilities with application for acoustic metamaterials. Soft Matter 14(2018) 6171–80.

[7] Cui S, Gong B, Ding Q, Sun Y, Ren F, Liu X, et al. Mechanical Metamaterials Foams with Tunable Negative Poisson's Ratio for Enhanced Energy Absorption and Damage Resistance. Materials 11(2018) 1869.

[8] Li Z, Wang X. On the dynamic behaviour of a two-dimensional elastic metamaterial system. International Journal of Solids and Structures 78–79 (2016) 174–81.

[9] Li J, Slesarenko V, Galich PI, Rudykh S. Oblique shear wave propagation in finitely deformed layered composites. Mechanics Research Communications 87(2018) 21–8.

[10] Gao C, Slesarenko V, Boyce MC, Rudykh S, Li Y. Instability-Induced Pattern Transformation in Soft Metamaterial with Hexagonal Networks for Tunable Wave Propagation. Scientific Reports 8(2018) 11834

[11] Christensen J, de Abajo FJG. Anisotropic Metamaterials for Full Control of Acoustic Waves. Physical Review Letters 108(2012) 124301.

[12] Slesarenko V, Galich PI, Li J, Fang NX, Rudykh S. Foreshadowing elastic instabilities by negative group velocity in soft composites. Applied Physics Letters 113(2018) 031901.

[13] Li J, Fok L, Yin X, Bartal G, Zhang X. Experimental demonstration of an acoustic magnifying hyperlens. Nature Materials 8(2009) 931–4.

[14] D. Nanda Kumar, G. Suganya, L.Nagarajan, Evaluation of Mechanical Properties of Bamboo/Epoxy Modified with Nanoclay Composites. SSRG International Journal of Mechanical Engineering 8.3(2021) 11-15.

[15] Mamaru Wutabachew, Dr. Negash Alemu. Investigation of Mechanical Properties of Horse Hair And Glass Fiber Rein Forced Hybrid Polymer Composite. SSRG International Journal of Mechanical Engineering 6.5(2019) 32-40.

[16] Madan Morle, Alok Agrawal. Physical and Mechanical Properties of Micro-Size Ceramic Particulate Filled Epoxy Composites. SSRG International Journal of Mechanical Engineering 6.9(2019) 23-26.

[17] Tang Y, Lin G, Han L, Qiu S, Yang S, Yin J. Design of Hierarchically Cut Hinges for Highly Stretchable and Reconfigurable Metamaterials with Enhanced Strength. Advanced Materials 27(2015) 7181–90.

[18] Overvelde JTB, Weaver JC, Hoberman C, Bertoldi K. Rational design of reconfigurable prismatic architected materials. Nature 541(2017) 347–52.

[19] Silverberg JL, Evans AA, McLeod L, Hayward RC, Hull T, Santangelo CD, et al. Using origami design principles to fold reprogrammable mechanical metamaterials. Science 345(2014) 647–50.

[20] Babaee S, Overvelde JTB, Chen ER, Tournat V, Bertoldi K. Reconfigurable origami-inspired acoustic waveguides. Sci Adv 2 (2016) e1601019.

[21] Triantafyllidis N, Maker BN. On the Comparison Between Microscopic and Macroscopic Instability Mechanisms in a Class of Fiber-Reinforced Composites. Journal of Applied Mechanics 52(1985) 794.

[22] Slesarenko V, Rudykh S. Microscopic and macroscopic instabilities in hyperelastic fiber composites. Journal of the Mechanics and Physics of Solids 99(2017) 471–82.

[23] Slesarenko V, Rudykh S. Harnessing viscoelasticity and instabilities for tuning wavy patterns in soft layered composites. Soft Matter 12 (2016) 3677–82.

[24] Galich PI, Slesarenko V, Li J, Rudykh S. Elastic instabilities and shear waves in hyperelastic composites with various periodic fiber arrangements. International Journal of Engineering Science 130(2018) 51–61.

[25] Shim J, Shan S, Košmrlj A, Kang SH, Chen ER, Weaver JC, et al. Harnessing instabilities for design of soft reconfigurable auxetic/chiral materials. Soft Matter 9(2013) 8198–202.

[26] Florijn B, Coulais C, van Hecke M. Programmable Mechanical Metamaterials. Physical Review Letters 113(2014) 175503.

[27] Li J, Arora N, Rudykh S. Elastic instabilities, microstructure transformations, and pattern formations in soft materials. Current Opinion in Solid State and Materials Science 25(2021) 100898.

[28] Bertoldi K, Boyce MC. Mechanically triggered transformations of phononic band gaps in periodic elastomeric structures. Physical Review B 77(2008) 052105.

[29] Tunable microstructure transformations and auxetic behavior in 3D-printed multiphase composites: The role of inclusion distribution. Composites Part B: Engineering 172(2019) 352–62.
[30] Bertoldi K, Boyce MC. Wave propagation and instabilities in monolithic and periodically structured elastomeric materials undergoing large deformations. Physical Review B 78(2008) 184107.
[31] Galich PI, Thomas E. Soft modes in nonlinear composites on the edge of elastic instability. Proc. of 26th International Congress on Sound and Vibration, (2019).
[32] Li J, Slesarenko V, Galich PI, Rudykh S. Instabilities and pattern formations in 3D-printed deformable fiber composites. Composites Part B: Engineering 148(2018) 114–22.
[33] Li J, Pallicity TD, Slesarenko V, Goshkoderia A, Rudykh S. Domain Formations and Pattern Transitions via Instabilities in Soft Heterogeneous Materials. Advanced Materials 31(2019) 1807309.
[34] Li J, Slesarenko V, Rudykh S. Microscopic instabilities and elastic wave propagation in finitely deformed laminates with compressible hyperelastic phases. European Journal of Mechanics, A/Solids 73 (2019) 126–36.
[35] Arora N, Li J, Slesarenko V, Rudykh S. Microscopic and long-wave instabilities in 3D fiber composites with non-Gaussian hyperelastic phases. International Journal of Engineering Science 157 (2020) 1034008.
[36] Bertoldi K. Harnessing Instabilities to Design Tunable Architected Cellular Materials. Annual Review of Materials Research 47(2017) 51–61.
[37] Samad Gadiwale, S. A. Kore. Analysis of Welded Joint Used in Pipeline Support Using Finite Element Method. SSRG International Journal of Mechanical Engineering 7.6(2020) 41-46.
[38] He Y, Zhou Y, Liu Z, Liew KM. Buckling and pattern transformation of modified periodic lattice structures. Extreme Mechanics Letters (2018) 112-21.